Princeton Plasma Physics Laboratory

PPPL- 4907

PPPL- 4907

Heating and Current Drive Requirements towards Steady State Operation in ITER

F.M. Poli, P.T. Bonoli, C.E. Kessel, D.B. Batchelor, M. Gorelenkova,
B. Harvey and Y. Petrov

June, 2013

PPPL PRINCETON PLASMA PHYSICS LABORATORY

Prepared for the U.S. Department of Energy under Contract DE-AC02-09CH11466.

Princeton Plasma Physics Laboratory
Report Disclaimers

Full Legal Disclaimer

Trademark Disclaimer

PPPL Report Availability

Princeton Plasma Physics Laboratory:

http://www.pppl.gov/techreports.cfm

Office of Scientific and Technical Information (OSTI):

http://www.osti.gov/bridge

Related Links:

U.S. Department of Energy

Office of Scientific and Technical Information

Fusion Links

Heating and current drive requirements towards Steady State operation in ITER

F.M. Poli*, P.T. Bonoli†, C.E. Kessel*, D. B. Batchelor**, M. Gorelenkova*, B. Harvey‡ and Y. Petrov‡

*Princeton Plasma Physics Laboratory, Princeton, NJ, 08543, USA
†Plasma Science Fusion Center, MIT, Cambridge, MA, xxxx, USA
** USA
‡CompX, Box 2672, Del Mar, CA 92014, USA

Abstract. Steady state scenarios envisaged for ITER aim at optimizing the bootstrap current, while maintaining sufficient confinement and stability to provide the necessary fusion yield. Non-inductive scenarios will need to operate with Internal Transport Barriers (ITBs) in order to reach adequate fusion gain at typical currents of 9 MA. However, the large pressure gradients associated with ITBs in regions of weak or negative magnetic shear can be conducive to ideal MHD instabilities, reducing the no-wall limit. The $E \times B$ flow shear from toroidal plasma rotation is expected to be low in ITER, with a major role in the ITB dynamics being played by magnetic geometry. Combinations of H/CD sources that maintain reverse or weak magnetic shear profiles throughout the discharge are the focus of this work. Time-dependent transport simulations indicate that, with a trade-off of the EC equatorial and upper launcher, the formation and sustainment of quasi-steady state ITBs could be demonstrated in ITER with the baseline heating configuration. However, with proper constraints from peeling-ballooning theory on the pedestal width and height, the fusion gain and the maximum non-inductive current are below the ITER target. Upgrades of the heating and current drive system in ITER, like the use of Lower Hybrid current drive, could overcome these limitations, sustaining higher non-inductive current and confinement, more expanded ITBs which are ideal MHD stable.

Keywords: steady state, ITER, ITBs, transport, current drive, heating, confinement
PACS: 52.25.Xz, 52.50.Sw, 52.50.Gj, 52.55.Fa, 52.65.-y

INTRODUCTION

One of ITER's legacies is the demonstration of continuous operation using non-inductive current drive. These advanced scenario plasmas operate at a plasma current lower than the baseline configuration (the 15 MA ELMy H-mode inductive scenario), to minimize the external heating power and current drive requirements [1].

The ITER steady state scenario targets plasmas with currents of 8-9 MA in the flat-top, with significant bootstrap current, self-generated by pressure gradients in magnetic field geometry [2]. Since the fraction of bootstrap current scales as $\beta_N q_{95}$, it is maximized at low current and high normalized pressure $\beta_N = \beta(aB_0/I_P)$, with I_P[MA] the total current, B_0[T] the magnetic field, a[m] the minor radius and β the ratio of the volume averaged plasma thermal energy to the magnetic energy. It has been estimated that, to compensate for the confinement degradation that occurs with decreasing plasma current and to get a fusion gain $Q = 5$ at a current of 9 MA, steady state operations should achieve $\beta_N > 2.5$ with a confinement gain factor $H_{98} > 1.5$ [3]. This implies regimes with improved core confinement, or Internal Transport Barriers (ITBs). However, the large pressure gradients associated with ITBs in regions of weak or negative magnetic shear may drive ideal MHD instabilities in a wide range of β_N, reducing the no-wall limits. The goal is to sustain moderate ITBs, with broad temperature and density profiles, with foot at mid-radius and beyond. These profiles have been observed in experiments with off-axis heating and current drive and weakly reversed to zero magnetic shear in the core (see [1, 4, 5] for a review).

Extrapolating present day ITB experiments to ITER is challenging because of the limited database available for densities close to the Greenwald limit and for ion and electron temperatures of comparable values. From present experiments with dominant electron heating, it is observed that magnetic shear reversed in the core is necessary for formation of ITBs in the electron channel, which have their foot locked at the radius of the minimum safety factor [4]. Confinement gain values higher than $H_{98} > 1.5$ have been demonstrated experimentally and routinely obtained on JT-60U high-β_P plasmas. For example, stable operation with $H_{98} \sim 1.6$, $\beta_N \sim 2.5$, weak reversed magnetic shear, an internal transport barrier at $r/a \sim 3/4$, and with 70-80% of non-inductive current drive (1/3 NB and 2/3 bootstrap)

have been demonstrated on JT-60U [6].

The JT-60U experiments indicate that performance can be improved by forming ITBs in the early ramp-up phase [7]. Heating in the ramp-up phase delays the inductive current penetration and favors the formation of magnetic shear profiles reversed in the core, which - in turn - favors the formation of ITBs. These results are used as guidelines in the simulations presented herein. The goal is to trigger ITBs in the early ramp-up phase, before the L-H transition, and sustain large confinement levels in the flattop, as well as a stationary, non-inductive current until the end of the burning phase. The scenario simulations discussed herein aim at maintaining weakly reversed in the core to flat magnetic shear profiles, minimum safety factor at mid-radius and higher than 2. Previous scenario simulations on a set of steady state configurations showed in fact that ideal MHD stable equilibria can be obtained operating with moderate ITBs that have their foot at mid-radius and with safety factor profiles that maintain $q_{min} > 2$ [8]. It will be shown that ITB formation and sustainment can be demonstrated with the baseline heating mix, but that LHCD is needed towards the ITER goals, to sustain higher current and confinement as well as more expanded ITBs.

SCENARIO DEVELOPMENT

Full plasma discharges are simulated with the Tokamak Simulation Code (TSC) [9], a predictive, free boundary transport evolution code. The plasma equilibrium and field evolution equations are solved on a two-dimensional Cartesian grid, while the surface-averaged transport equations for the pressure and densities are solved in magnetic flux coordinates.

TSC includes a 2D representation of the central solenoid, of the poloidal field coils and of the surrounding conducting structures, as well as feedback systems for plasma position, shape and current. TSC is used to establish the scenario in terms of all parameters as a function of time, targeting the desired properties of the scenario and attempting to remain within all limits.

Particle transport models are not used, instead the electron density profiles are prescribed, as the superposition of a broad profile for the H-mode and a peaked profile that imitates the ITB. The Helium concentration is determined by an input $\tau^*_{\mathrm{He}}/\tau_{\mathrm{E}} = 5$ and includes the buildup to burn conditions. The Hydrogen (DT) fuel density is determined from quasi-neutrality assuming equal amounts of D and T. The impurity density profiles are assumed to be the same as the electron density, with their fractions prescribed as a function of time. Dominant impurities are Beryllium (2% fraction of the electron density) and Argon (0.4% fraction), which provide about 18-40MW of core radiated power, depending on the current.

The external power heating sources considered in this work are 33 MW of negative ion neutral beam (NB), 20 MW of ion cyclotron (IC), 20MW of Electron Cyclotron (EC) and up to 40 MW of Lower Hybrid Current Drive (LH). The external heating starts at 15s, shortly after divert time, while the NB injection begins when admissible density is reached, at 75s. At this time the total external power is above the threshold for L-H transition, which is imposed by dropping the thermal diffusivity profile at the edge to form a pedestal. The width and the height of the pedestal are set by the EPED1 peeling-ballooning stability code [10]. A combination of two RF sources is used in L-mode, with power stepped-up to reach total 40MW at 75s to favor the transition time. The reference scenarios analyzed use 33MW of NB and include the baseline heating mix (20MW of EC + 20MW of IC), and two configurations with LH, one with 20MW each of EC and LH, the other with 20MW of IC (stepped down to 5MW in the flattop) and 40MW of LH.

The heating and current drive profiles are calculated using modules external to TSC, which are described below. This is done either within the SWIM framework or using TRANSP. In the former case TSC calls directly the H&CD codes and advances self-consistently the equilibrium and pressure profiles. In the second approach TSC provides experimental-like conditions: the equilibrium and pressure profiles are given to TRANSP, which calculates the H&CD profiles for the whole discharge. These are then given back to TSC for recalculation of the scenario, iterating the process a few times for convergence.

Ion cyclotron model. The Ion cyclotron heating is used in the ramp-up phase to provide heating and current in the core and to help with the L-H transition, then the IC power is stepped down in the flattop. The ICRH uses Helium-3 ion minority heating at a concentration of 2% of the electron density and a frequency of 48 MHz for on-axis deposition and to accommodate the strong magnetic axis shift. The ICRF source model is the TORIC full wave [11] with a Fokker Planck treatment of the resonant species and equivalent Maxwellian for other fast species (neutral beam ion and alpha particles).

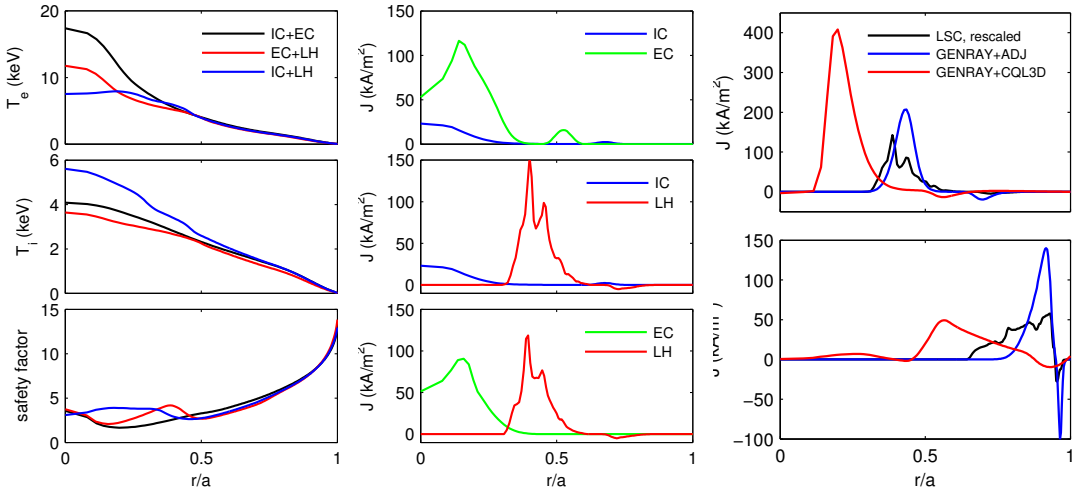

FIGURE 1. Left: temperature and safety factor profiles. Center: toroidal current density profiles, calculated at 67.5s, with the CDBM transport model and using the IPS framework. Right: LH toroidal current density, calculated at 30s (top) and 95s (bottom). Comparison between LSC rescaled by a factor 1.6, GENRAY with the adjoint current calculation and GENRAY with the 2D Fokkep Planck CQL3D.

Neutral beam model. The NB source model is the NUBEAM orbit following Monte Carlo [12, 13]. The NB has 1 MeV particle energy, with the capability to steer from on-axis to off-axis. The deposition profiles peak at normalized radius $\rho \sim 0.25 - 0.35$ depending on the steering angle, providing up to ~ 3 MA of non-inductive current. It is found that keeping one beam on-axis does affect the evolution of the current profile in the first 500s of the discharge, limiting the increase of $q(0)$ and preventing the formation of a current hole. All simulations shown herein use one beam on-axis and one-beam off-axis.

Electron cyclotron model. The electron cyclotron heating and current drive are calculated either with TORAY [14] (when using TRANSP) or GENRAY [15, 16] (when using the SWIM framework), both ray-tracing 1D Fokker Planck codes, which include relativistic effects, electron-ion collisions and trapped particle effects. The ITER electron cyclotron system will use 20MW in its baseline configuration for heating and current drive, which can be diverted to either an equatorial launcher (EL) or an upper launcher (UL) by means of a switch in the transmission line [17]. The EL has three lines of injection, of which the middle line will be injecting waves in the counter-current drive direction. The UL has highly localized off-axis deposition at $\rho = 0.45 - 0.8$ and can delivered the full 20MW distributing the power in two rows: an upper (USM) and a lower (LSM) steering mirror [17, 18]. Compared to the other sources the EC has unique flexibility for deposition control. In this work, both the equatorial and the upper launcher are used aiming at optimizing the current profile for ITB formation and sustainment.

Lower Hybrid heating and current drive. Among the RF sources, the LH has the highest current drive efficiency and it deposits far off-axis, where is more needed for keeping the ITB foot at large radii. TSC can calculate the heating and current drive profiles internally, using the 1D Fokker Planck LSC code [19], or call GENRAY within the SWIM framework. The LSC code underestimates the driven current by a factor of 1.6 in the flattop phase, according to simulations run with GENRAY+CQL3D [20] (2D Fokker-Planck) on single time slice [21]. To account for this factor, the power spectrum is modified from the reference weighting 72.5% forward and 27.5% backward to 87% forward and 13% backward power weighting when using LSC and the driven current scaled consistently [21].

FORMATION OF INTERNAL TRANSPORT BARRIERS

To study the ITB formation and dynamics we use the CDBM (Current Diffusive Ballooning Mode) model [22], which has been extensively applied to the interpretation of ITBs on JT-60U in NB, EC and LH heated plasmas. This transport model is based on the theory of self-sustained turbulence due to current diffusivity driven modes [23]. It includes a

term for turbulence reduction due to weak or negative magnetic shear and large Shafranov shift effect. The total MHD pressure term, which includes the fast ion pressure, is taken into account in the calculation of the thermal diffusivity [24]. An additional term to account for the $\mathbf{E} \times \mathbf{B}$ flow shear stabilization is also included in the calculation of the thermal diffusivity, although is a small correction to the thermal diffusivity profile for the scenarios under study. Since the CDBM model is a core model, we use it for $\rho \leq 0.75$ and combine at the edge with a modified Coppi-Tang model and with an analytic form for the pedestal [25].

Figure 1 shows the profiles of safety factor, ion and electron temperature calculated in L-mode, at 67s, before the L-H transition time (which occurs at 75s). The figure compares a configuration with IC and EC and two configurations with LH, combined respectively with EC and with IC. All simulations have been run with the Integrated Plasma Simulator and use the LSC ray tracing code for the LH calculations. A comparison with GENRAY and with CQL3D is shown in the last column of Fig.1 for the scenario simulation with 20MW of EC and 20MW of LH.

At the low density and current in the early ramp-up phase, all combinations of sources can form magnetic shear profiles either reversed in the core or flat in L-mode. The strongest ITBs are those triggered in the baseline heating configuration. Both IC and EC deposit at about $\rho \simeq 0.2$ and this set a global minimum in the safety factor profile. This configuration has been extensively discussed in a previous work, where it was shown that ITB formation is favored by using the equatorial launcher in the ramp-up, while ITB sustainment and larger bootstrap current are favored by switching to the upper launcher at the beginning of the flattop phase, yet keeping one third of the power on the equatorial launcher [25]. The top and bottom injection lines of the EC equatorial launcher are aiming 5 degrees towards the equatorial plane, since this steering configuration was found to be favorable to the sustainment of reverse shear profiles in the ramp-up phase. The poloidal angle is tilted by 10 degrees, thus aiming 5 degrees away from the equatorial plane at the end of the ramp-up phase. The same steering configuration is also used in the scenario with EC+LH.

In the other two configurations the sources do not deposit at the same radial region and this causes the formation of two local minima in the safety factor profile. The CDBM model responds to these minima steepening the temperature gradient locally, but the effect is weaker than in the configuration with IC+EC and the reduction in the transport in the core is smaller.

However, tilting the poloidal steering angle of the equatorial launcher to deposit off-axis does not help. In fact, simulations indicate that the electron temperature drops by about 60% in the core, at $\rho \leq 0.3$ and hollow profiles form. These results suggest that core electron heating in the early ramp-up phase is important for reverse shear formation in the core and for triggering strong ITBs. A combination of IC heating and core EC heating can provide such an environment.

The last column in Fig.1 shows a comparison between deposition profiles calculated with the IPS framework using LSC, GENRAY and GENRAY+CQL3D. The profiles are calculated in the ramp-up at two times, 30s and 90s. At the low densities of start-up, the quasilinear plateau is completely flat and this greatly reduces the damping. As the density increases, the collisional restoration of the distribution function to a Maxwellian starts to counteract the quasilinear flattening and more of a slope develops in the distribution function which gives more damping. This is observed as deposition profiles that are peaked at lower radii, since the LH waves penetrate deeper before being absorbed. With increasing density in the ramp-up phase, the damping moves outward.

TOWARDS STATIONARY SOLUTIONS WITH ITB

Figure 2 shows the safety factor, ion and electron temperature profiles in the relaxed phase, at 2900s, for the same heating mixes discussed in the previous section. The flattop relaxed plasma parameters are reported in Table I. In the baseline configuration (20MW of EC and 20MW of IC) 6.7MW of EC power are switched from the equatorial launcher to the upper launcher at the beginning of the flattop phase. The lower current drive efficiency of the upper launcher is compensated by a larger bootstrap current and this steering configuration sustains higher non-inductive current than a configuration that delivers two third of power to the equatorial launcher, despite the higher current drive efficiency from the equatorial injection line [25].

The reverse current lobe from the LH in the two configurations with LH is reducing the height of the pedestal bootstrap current. This affects the safety factor profile at the edge, which does not develop a local minimum aligned with the maximum bootstrap current. This minimum in q has direct consequences on the ideal MHD stability of configurations with EC heating and current drive at high normalized pressure [8].

The configuration with 20MW of EC and 20MW of LH uses the same power distribution as the day-one heating mix, with two-third of the power to the upper launcher and one third to the equatorial launcher. However, the steering

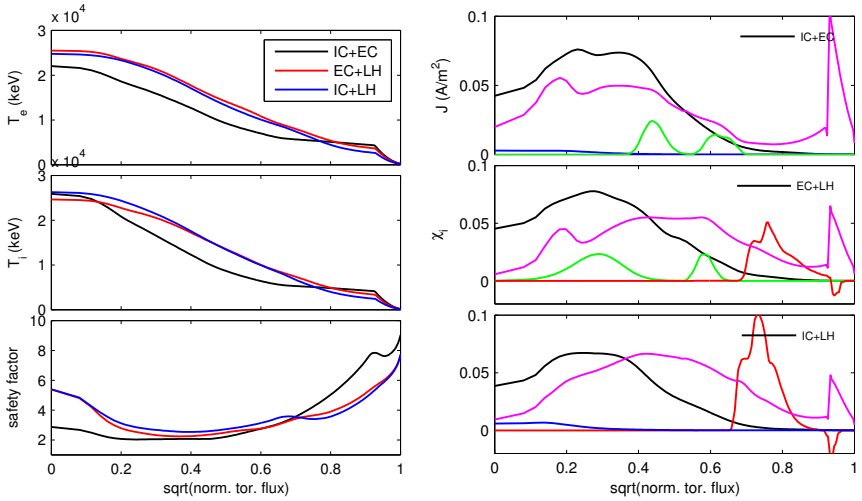

FIGURE 2. Left: temperature and safety factor profiles calculated at 2900s, for the same heating configurations shown in Fig.1. Right: toroidal current profiles, calculated at the same time.

angle of the equatorial launcher has been decreased in this case to deposit at lower radii.

With 78MW of injected power (40MW of LH, 33MW of NB and 5MW of IC in the flattop phase), the configuration with IC+40MW of LH sustains 250kA higher non-inductive current compared to the configuration with 20MW each of EC and LH (total 73MW). It has lower confinement and lower normalized pressure, but higher alpha power and fusion gain, as shown in Table I. The value of q_{95} is comparable and close to 6, but 40 MW of LH are more effective in modifying the current profile off-axis and this configuration has a secondary, weak, local minimum in the safety factor profile at $\rho \simeq 0.8$.

A main difference between the day-one heating mix and the two configurations with LHCD is that in the former case the temperature profiles are more peaked and the confinement is lower. The ITB foot is at about $\rho \simeq 0.4$ and heating the ITB is more difficult. In fact, the EC should deposit inside the ITB, but this would make pressure profiles peaked, favoring the triggering of ideal MHD instabilities at moderate values of β_N, as discussed in [8, 25]. Expanding the ITB would be probably possible, with a real-time feedback of the EC steering angles and with a feedback on the position of the minimum safety factor.

Because of its higher current drive efficiency, the LH is more effective than the upper launcher in setting the ITB foot at large radii. Thus, in configurations with LHCD the EC deposits inside the barrier and is more effective in controlling the current profile. As shown in Fig.2 the bootstrap current profiles are broader and peaked at mid-radius.

All three heating configurations sustain stationary current in the flat-top phase, almost zero to strong reverse shear and ITBs until the end of the flattop phase. However, none of them reaches the ITER goals of 9MA and $Q = 5$.

TOWARDS THE ITER GOAL OF 9MA AND Q=5

The dimensionless parameter $H_{89}\beta_N/q_{95}^2$ is a measure of the performance in a tokamak, which is affected by three key parameters: the confinement, the pressure limit and the limit to increasing plasma current [1]. Confinement and bootstrap current can be improved by increasing the Greenwald fraction and optimizing the current profile. For example, the configuration with 20MW each of EC and LH can increase the bootstrap fraction from 50% to 56% by operating at the Greenwald density. This configuration also increases the normalized pressure to $\beta_N = 2.4$, the confinement to $H_{98} = 1.53$ and the fusion gain to $Q = 3.3$. The minimum safety factor stays above 2, which makes these plasmas ideal MHD stable to the $n = 1$ kink mode.

Using the same heating mix and the same density profile, but applying a modified Coppi-Tang model we find that the configuration with 20MW each of EC and LH can sustain 9MA provided $H_{98} = 1.6$. Interestingly, for the same confinement gain, also the CDBM model predicts a non-inductive current of 9MA, indicating that confinement improvement is a necessary condition towards the ITER goals.

TABLE 1. Plasma parameters calculated at $t = 2500\,\mathrm{s}$. The first column refers to the baseline configuration, the second column replaces IC with LH and keeps the same level of EC and NB heating. The last two columns show configurations where the LH power is progressively increased to 30MW and to 40MW Quantities in bold fonts are input to TSC, like the requested plasma current waveform I_P.

NB (MW)	33	33	33	33	33
IC (MW)	20→15	/	20→5	/	/
EC (MW)	20	20	/	20→13.4	20→ 6.7
LH (MW)	/	20	40	30	40
$\mathbf{I_P}$ (MA)	6.5	8.0	8.2	8.7	9.0
I_NI (MA)	6.2	8.06	8.3	8.6	9.12
I_BS (MA)	3.3	4.07	4.25	4.88	5.0
I_NB (MA)	2.4	2.5	2.47	2.0	2.19
I_EC (MA)	0.36	0.45	/	0.35	0.149
I_LH (MA)	/	0.95	1.64	1.23	1.67
P_α	22	40	46	62	64
Q	1.62	2.75	2.92	4.0	4.0
n/n_G	1.0	0.91	0.97	1.0	1.0
$T(0)$ (keV)	21.8	25.4	24.3	27.4	25.8
$l_i(1)$	0.97	0.80	0.79	0.77	0.69
$q(0)$	2.9	5.6	7.8	5.4	5.8
q_{95}	7.7	6.0	5.98	5.6	5.3
β_N	1.6	2.05	1.96	2.05	1.87
H_{98}	1.32	1.44	1.36	1.52	1.44

Table I compares the reference heating mix discussed in the previous section with two upgrades of the configuration that uses EC+LH, where the LH injected power is progressively increased to 30MW and to 40MW. At the same time the total EC power has been reduced in the flattop in order to maintain the total power load to the divertor below 100MW. The configuration with 30MW of LH uses thus 13.4MW of EC power from the equatorial launcher, while the configuration with 40MW of LH uses 6.7MW of EC from the lower injection line of the equatorial launcher. The total external power is therefore increased from 73MW in the configuration with 20MW of LH to 76.4MW in the configuration with 30MW of LH up to 79.7MW in the configuration with 40MW of LH. All these upgrade configurations operate at the Greenwald fraction. Increasing the LH injected power from 20 to 30MW increases the non-inductive current up to 8.6MA and the fusion gain to $Q = 4$. Further increase of the LH power does not significantly improve the scenario. Despite the current being now just above the target 9MA, there is no improvement in the confinement or in the fusion gain. However, it should be noted that no systematic scan of the EC steering angle has been done to optimize the bootstrap current and to improve the performance of this scenario.

The CDBM model predicts that 40MW of LH do not sustain 9MA of non-inductive current when combined with 5MW of IC in the flattop, but they do when combined with 6.7MW of EC. The difference in the non-inductive current is about 700kA and it is due mainly to a difference in the bootstrap current rather than to the lower current drive efficiency of IC compared to EC. In fact, the difference between the IC and the EC driven current is only 100kA, while the gain in bootstrap current is about 450kA in the configuration that uses EC, indicating that combining EC with LH in the flattop is a promising route towards the demonstration of steady state operation in ITER.

The EC is the most flexible source, because it can deposit where other sources cannot, between 0.35 and 0.65 of the normalized radius. It can therefore be valuable in controlling the current and pressure profile, which is a key feature for steady state operation. However, simulations indicate that its effectiveness depends on the synergy with other heating and current drive sources. In configurations with EC only, temperature profiles are peaked and the current profiles are stiff to the steering angle configuration [25]. In configuration with LH, instead, the LH sets the ITB foot at larger radii making the EC more effective in modifying the current profiles and in maintaining bootstrap current profiles broad and peaked at mid-radius.

CONCLUSIONS

The ITER steady state scenario is significantly dependent on the heating and current drive sources, since the current profiles, in combination with the bootstrap current, determine the safety factor profile. In order to achieve the goal of $Q = 5$ at a non-inductive current between 8MA and 9MA, ITER steady state will need to sustain bootstrap fraction of 0.5-0.7 and improve the energy confinement times above 50% of the H-mode values. This will likely be obtainable only in regimes with Internal Transport Barriers.

The heating and current drive sources planned for ITER should be capable of triggering ITBs in the early discharge phase and to sustain them in the flattop, as well as sustaining a stationary, 100% non-inductive current. At the same time, the sources should sustain a weakly reversed shear in the core (to avoid strong ITB), and have enough flexibility to control the position of the minimum safety factor (which sets the ITB foot position in reversed shear magnetic equilibria) and to sustain broad bootstrap current profiles with maximum at mid-radius.

In this work we have analyzed various combinations of heating and current drive sources with focus on their capability to trigger ITBs in the ramp-up phase, sustain them in the flattop and improve plasma performance towards the steady state goals. Previous analysis on the ideal MHD stability limits have been used as a reference to develop scenarios that maintain the plasma in the ideal MHD stable region.

The scenario simulations indicate that:

- by trading-off the power between the equatorial and the upper launcher, the day-one heating mix can trigger ITBs in L-mode by reverse magnetic shear formation in the core and sustain them in the flat-top phase for the whole burning phase, by maintaining weakly reversed magnetic shear profiles. The non-inductive current and the fusion gain are well below the ITER goals, but this configuration is MHD stable around the operating point for variations of 10% of the Greenwald fraction and of the pressure peaking factor. It can be therefore a good candidate for demonstration of steady state operation at low current of about 7MA.
- the use of LHCD is necessary for achievement of higher confinement, sustainment of higher non-inductive current and higher fusion gain. Non only the LH has higher current drive efficiency and it deposits in the outer mid-radius, where is needed, but it is effective in decreasing the safety factor at the edge and in setting and maintaining the ITB foot at larger radii. The reverse current lobe of the LH reduces the bootstrap current at the edge, avoiding the formation of a localized and deep minimum in the q profile at the edge, which instead forms in configurations that use EC only.
- Although 33MW of NB and up to 40MW of LH are necessary for the sustainment of 9MA of non-inductive current, the use of higher current drive efficiency sources is not a sufficient condition. The H&CD sources should be able to distribute the current broadly over the minor radius. The EC source has the greatest flexibility to this purpose, since can deposit where other sources cannot. We find that 40MW of LH and 33MW of NB cannot sustain 9MA non-inductively when combined with 5MW of IC in the flattop, but they can when combined with as low as 6.7MW of EC. By combining EC and LH, in fact, not only sets the ITB foot at large radii, which is necessary for ideal MHD stability, but enhance the effectiveness of the EC source in successfully modifying the current profile and maintaining broad bootstrap current profiles, thus improving the confinement.

There are in general several sources of uncertainties in scenarios simulation results. In the absence of a benchmarked particle transport model, density profiles are usually prescribed, in this case as a function of time and a transport model is used to evolve the temperature profile. Results are therefore affected by hypotheses on the density profiles and on the transport model chosen. Transport models that are used for the simulation of the ITER baseline and of the hybrid scenarios do not respond to magnetic reverse shear and therefore fail when applied to the steady state configurations, which rely on reverse shear maintainance for ITB formation and sustainment. Another uncertainty in the results is represented by the actuator models used to predict heating and current drive profiles. We find, for example, that quasi-linear effects can modify the deposition profile of the LH source and that these effects are larger at the low densities typical of the ramp-up phase.

It is important that hypotheses are benchmarked against the available transport codes and verified experimentally in present day tokamaks, in dedicated experiments that target steady state accessibility.

ACKNOWLEDGMENTS

This work was supported by the US Department of Energy under contract DE-AC02-CH0911466.

REFERENCES

1. C. Gormezano, A. C. C. Sips, T. C. Luce, S. Ide, A. Becoulet, X. Litaudon, A. Isayama, J. Hobirk, M. R. Wade, T. Oikawa, R. Prater, A. Zvonkov, B. Lloyd, T. Suzuki, E. Barbato, P. Bonoli, C. K. Phillips, V. Vdovin, E. Joffrin, T. Casper, J. Ferron, D. MAzon, D. Moreau, R. Budny, C. Kessel, A. Fukuyama, N. Hayashi, F. Imbeaus, M. Murakami, A. R. Polevoi, and H. E. S. John, *Nucl. Fusion* **47**, S285 (2007).
2. R. J. Bickerton, J. W. Connor, and J. B. Taylor, *Nature Phys. Sci.* **229**, 110 (1971).
3. Y. Shimomura, Y. Murakami, A. R. Polevoi, P. Barabaschi, V. Mukhovatov, and M. Shimada, *Plasma Phys. Control. Fusion* **43**, A385 (2001).
4. J. W. Connor, T. Fukuda, X. Garbet, C. Gormezano, V. Mukhovatov, M. Wakatani, the ITB Database Group, and the ITPA Topical Group on Transport and Internal Transport Barrier Physics, *Nucl. Fusion* **41**, 1823 (2001).
5. R. C. Wolf, *Plasma Phys. Control. Fusion* **45**, R1–R91 (2003).
6. Y. Kamada, *Plasma Phys. Control. Fusion* **42**, A65 (2000).
7. S. Ide, and the JT-60U team, *J. Plasma Fusion Res. SERIES* **4**, 99 (2001).
8. F. M. Poli, C. E. Kessel, M. S. Chance, S. J. Jardin, and J. Manickam, *Nucl. Fusion* **52**, 063027 (2012).
9. S. C. Jardin, J. L. Delucia, and N. Pomphrey, *J. Comput. Phys.* **66**, 481 (1986).
10. P. B. Snyder, N. Aiba, M. Beurskens, R. J. Groebner, L. D. Horton, A. E. Hubbard, J. W. Hughes, G. Huysmans, Y. Kamada, A. Kirk, C. Konz, A. W. Leonard, J. Lonnroth, C. F. Maggi, R. Maingi, T. H. Osborne, N. Oyama, A. Pankin, S. Saarelma, G. Saibene, J. L. Terry, H. Urano, and H. R. Wilson, *Nucl. Fusion* **49**, 085035 (2009).
11. M. Brambilla, A full wave code for ion cyclotron waves in toroidal plasmas, Rep. IPP 5/66 5/66, Max-Planck-Institut fur Plasmaphysik, Garching, Computer Science Department, Fanstord, California (1996).
12. R. J. Goldston, D. C. McCune, H. H. Towner, S. L. Davis, R. J. Hawryluk, and G. L. Schmidt, *J. Comput. Phys.* **43**, 61 (1981).
13. A. Pankin, D. McCune, R. Andre, G. Bateman, and A. Kritz, *Comput. Phys. Commun.* **159**, 157 (2004).
14. A. H. Kritz, H. Hsuan, R. C. Goldfinger, and D. B. Batchelor, "Heating in Toroidal plasmas," in *Proc. 3rd Joint Varenna-Grenoble Int. Symp., Grenoble*, edited by CEC, IAEA, Brussels, 1982, vol. 2, p. 707.
15. R. W. Harvey, and M. G. McCoy, "," in *Proceedings of the IAEA Technical Committee on Advances in Simulation and Modeling of Thermonuclear plasmas*, IAEA, Vienna, 1993, p. 489.
16. A. S. et al, "," in *Proceedings of the 15th Workshop on ECE and ECRH*, World scientific, 2009, p. 301.
17. M. A. Henderson, R. Chavan, R. Bertizzolo, D. Campbell, J. Duron, F. Dolizy, R. Heidinger, J.-D. Landis, G. Saibene, F. Sanchez, A. Serikov, H. Shidara, and P. Spaeh, *Fusion Science and Technology* **53**, 139 (2008).
18. G. Ramponi, D. Farina, M. A. Henderson, E. Poli, G. Saibene, and H. Zohm., *Fusion Science and Technology* **52**, 193 (2007).
19. D. W. Ignat, *Nucl. Fusion* **34**, 837 (1994).
20. R. W. H. et al, "," in *Proceedings of the 38th EPS Conf. on Plasma Phys.*, IOP, 2011, p. P4.017.
21. C. E. Kessel, A. H. Kritz, T. Rafiq, G. Bateman, D. McCune, R. Budny, D. Campbell, T. Casper, Y. Gribov, and J. Snipes, "Development of the ITER Advanced Steady State and Hybrid Scenarios," Vienna:IAEA, 2010, vol. ITER/P1-22, `http://www-pub.iaea.org/mtcd/meetings/cn180papers.asp`.
22. A. Fukuyama, K. Itoh, S.-I. Itoh, M. Yagi, and M. Azumi, *Plasma Phys. Control. Fusion* **37**, 611 (1995).
23. K. Itoh, M. Yagi, S.-I. Itoh, A. Fukuyama, and M. Azumi, *Plasma Phys. Control. Fusion* **35**, 543 (1993).
24. *Modification of CDBM trransport model and its impact on JT-60U experimental analysis and ITER predictio*n, presented at the 8th ITPA-IOS meeting, Apr 2012, Madrid (????).
25. F. M. Poli, and C. E. Kessel, *Phys. Plasmas* **20**, 056105 (2013).

The Princeton Plasma Physics Laboratory is operated
by Princeton University under contract
with the U.S. Department of Energy.

Information Services
Princeton Plasma Physics Laboratory
P.O. Box 451
Princeton, NJ 08543

Phone: 609-243-2245
Fax: 609-243-2751
e-mail: pppl_info@pppl.gov
Internet Address: http://www.pppl.gov